



Economic limitation of recent heterogeneous catalysts for ammonia synthesis

Masaki Yoshida¹, Takaya Ogawa^{*,1}, Keiichi N. Ishihara

Graduate School of Energy Science, Kyoto University, Yoshida-honmachi, Sakyo-ku, Kyoto 606-8501, Japan

ARTICLE INFO

Keywords:

Cost analysis
Process simulation
Newly developed catalyst for ammonia synthesis
Ruthenium catalyst

ABSTRACT

The economic performance of newly developed catalysts for ammonia synthesis, Ru/Ca(NH₂)₂ and Ru/Pr₂O₃, are evaluated by process simulation using Aspen Plus®. The results show that the high activity of the new catalysts reduces the electricity cost for pressurizing reactant gases; however, the electricity for lowering the temperature in ammonia separation through liquefaction is significant due to the mitigated pressure and almost compensates for the decreased cost. The results show an economic limitation to current research trends that develop a catalyst for ammonia synthesis under low pressure. It is noted that catalyst costs are high due to expensive ruthenium; thus, the lifetime of catalysts significantly influences the total cost. With the assumption of a long lifetime of catalysts, the new catalysts are advantageous when the electricity cost is high, the characteristics of the case in which renewable energy is employed. As the future direction of the catalyst development, recycling or extending the lifetime of the catalysts and replacing Ru with cheap metal will be crucial from the economic viewpoint. Moreover, effective methods for ammonia collection, such as adsorbents, should be focused on reducing the electricity of ammonia liquefaction in cooling separation and giving a vital meaning to the condition mitigated by the newly developed catalysts.

1. Introduction

Ammonia is inevitable for modern human lives as an artificial nitrogen fertilizer, and it is the second most common chemical produced worldwide (U.S. Geological Survey 2020). In 2019, the total ammonia production reached >182 million tonnes, which is expected to increase by 2.3 % per year (Morlanés et al., 2021). Ammonia synthesis occupies 1–2 % of the whole energy consumption of human beings, indicating an enormous energy-consuming process (U.S. Energy Information Administration 2020). Currently, fossil fuels are the sources of hydrogen and energy for industrial ammonia production (Liu, 2013). Thus, for a sustainable society in the future, “green ammonia” should be synthesized from the hydrogen gas prepared by water electrolysis based on renewable energy.

Moreover, ammonia is a potential renewable energy carrier since it readily transforms in a liquid state at <10 bar at room temperature, and liquid ammonia has a high energy density in weight and volume (Lamb et al., 2019; Kojima, 2019; Lan et al., 2012; Wijayanta et al., 2019). Ammonia-fueled power generation technology is being established

(Zhao et al., 2019; Kobayashi et al., 2019). The smaller volume results in less space in the fuel tank, and the smaller weight requires less energy to transport fuels together. Furthermore, nitrogen gas is the product of ammonia after usage, and it can be emitted into the air without pollution. Moreover, nitrogen gas can be obtained from the air everywhere. This means that after utilizing ammonia, there is no need to recover and send back nitrogen gas to the location that generates hydrogen from renewable energy, omitting the cost and energy for recovery and transportation (Sgouridis et al., 2019; Götz et al., 2016; Supekar and Skerlos, 2015; Ogawa, 2022). Therefore, liquid ammonia is suitable as a portable fuel and is beneficial to supply power for the transport sector, accounting for roughly 30 % of the world’s energy consumption (U.S. Energy Information Administration 2016). The market size of ammonia has an enormous potential to expand in the near future.

Ammonia is produced through an exothermic reaction: $N_2 + 3H_2 \rightarrow 2NH_3$ $\Delta H = -92$ kJ (Atkins et al., 2018). Therefore, the lower temperature and higher pressure are favorable in equilibrium. However, the temperature must be elevated (350–525 °C) to accelerate the reaction at extremely high pressure (100–300 bar) (Liu, 2014). The equipment,

* Corresponding author.

E-mail address: ogawa.takaya.8s@kyoto-u.ac.jp (T. Ogawa).

¹ M. Y. and T. O. contributed equally to this work.

including reactors and compressors, is then much more expensive to endure the severe condition. These costs are usually reduced by the economy of scale (Woods, 2007). Thus, the ammonia production of a plant is generally large, e.g., 1000 tonnes/day (Brown et al., 2014). The business model of centralized production and distribution to local areas has been successful for a long time. However, insufficient infrastructure for transport, such as feeder roads that link main cities to other regions of Zambia, Tanzania, Ghana, and Nigeria, increases the transaction cost, and farmers in these areas cannot obtain ammonia at an affordable price (Chauhan, 2018; *The World's Most Expensive Fertilizer Market: Sub-Saharan Africa 2016*). This results in low efficiency of food production, increasing the prevalence of hunger.

Furthermore, the harsh conditions require a significant time of at least 30 h for the start-up, (Donald and Robert, 1986; Paul et al., 1978) which is fatal to the utilization of renewable energy due to its time variability. If the synthesis of ammonia under mild reaction conditions is achieved, it would be possible to produce green ammonia using water and renewable energy and to employ ammonia as an energy carrier. Moreover, this enables producing ammonia locally on a small scale and supplying it to local areas without transport costs. Therefore, a mild reaction condition is essential to solve the above issues.

The catalysts for ammonia synthesis have been remarkably redeveloped in recent years, starting with the report of Ru supported by an electrone in 2012 (Kitano et al., 2012). Several catalysts supported on not only on electrides but also nitrides and hydrides or without supports have also been reported one after another, which have high activity under mild reaction conditions (Ye et al., 2020; Ogawa et al., 2018; Hattori et al., 2018; Wang et al., 2017; Wang et al., 2021; Kobayashi et al., 2017; Wu et al., 2019). Homogeneous catalysts for ammonia synthesis at room temperature and atmospheric pressure have been developed since 2003 (Yandulov and Schrock, 2003; Wickramasinghe et al., 2017; Arashiba et al., 2011; Ashida et al., 2019; Anderson et al., 2013; Chalkley et al., 2020). These catalysts are very promising in solving the abovementioned problems. However, to the best of our knowledge, no research has investigated how economically advantageous these catalysts are in a process that correctly reflects their surprisingly high performance. There are numerous examples of evaluating the performance of ammonia synthesis loops. However, they employ conventional iron-based catalysts or assume unrealistic catalytic activities, such as reaching equilibrium immediately or constant reaction activity under various conditions (Nosherwani and Neto, 2021; Frattini et al., 2016; Sánchez and Martín, 2018; Sánchez and Martín, 2018; Al-Zareer et al., 2018; Hasan and Dincer, 2019; Bicer et al., 2016; Araújo and Skogestad, 2008; Arora et al., 2016; Andersson and Lundgren, 2014). It is crucial to investigate the cost structure of the synthetic loops with recent catalysts to reveal the conditions they are advantageous, how they can be made more economically viable, and the direction for future catalyst development.

In this study, the economics of processes is evaluated incorporating the newly developed catalysts for ammonia synthesis. We focus on Ru/Ca(NH₂)₂ (Kitano et al., 2018) and Ru/Pr₂O₃, (Imamura et al., 2019) which show remarkable activity and for which experimental data are abundantly reported to enable reaction modeling. The Ru/Ca(NH₂)₂ has higher activity than Ru/Pr₂O₃, but the Ru content is twice: Ru/Ca(NH₂)₂ and Ru/Pr₂O₃ have 10 and 5 wt% of Ru, respectively. Thus, the comparison unravels which is critical to the cost: catalytic activity or Ru amount per weight. ASPEN Plus© was used to model the ammonia synthesis loops embedded with the two catalysts. A modified Temkin model was used to correctly assess their catalytic activity. In the reported paper, the available data were the test under the reaction conditions up to 10–30 bar, (Kitano et al., 2018; Imamura et al., 2019) but it is inferred that the target conditions for those catalysts are around 50 bar (Tsubame BHB Co. 2022). We extrapolated the low-pressure results and modeled them as data at 50 bar. The economic feasibility was evaluated at various scales, from small to large scale, and by varying the cases, such as using storage batteries to smooth out the time variability of

renewable energy. The results show an economic limitation to the current research trends that develop a catalyst for ammonia synthesis under low pressure. In addition, the conditions under which the newly developed catalyst shows superiority are clarified, and the directions for future catalyst development are discussed.

2. Method

2.1. Whole scheme of the ammonia synthesis loop

Fig. 1 shows the system boundary of this study. An ammonia production plant consists of hydrogen and nitrogen production and an ammonia synthesis loop. The ammonia synthesis loop was focused in this study because the purpose was to evaluate the impact of the mild reaction conditions achieved by Ru/Ca(NH₂)₂ and Ru/Pr₂O₃ on the ammonia synthesis loop. In addition, the loops with the commercialized iron-based catalyst (KM1R (Fe)) and conventional Ru-based catalyst (Ru/C) (Aika et al., 1972; Saadatjou et al., 2015; Aika, 2017) were also investigated as a comparison. Although the cost of the hydrogen and nitrogen production process is inevitable, it does not change the conclusion on the comparison among all plants because the amount of hydrogen and nitrogen gas is the same. Therefore, the cost calculation for the ammonia synthesis loop is sufficient for the comparison (Fig. 1).

Cryogenic air separation is suitable to prepare nitrogen gas due to the high purity of nitrogen, (Frattini et al., 2016; Smith and Klosek, 2001) since the catalysts for ammonia synthesis are readily poisoned by H₂O and O₂ (Rohr et al., 2019). Pressure swing adsorption is not suitable because it cannot achieve high purity for ammonia synthesis, although it seems preferable for small-scale production. We assumed to utilize the cold heat of N₂ in the cryogenic air separation to cool down ammonia for the separation. Aspen Plus© was used to simulate the whole process of the ammonia synthesis loop. The loop was based on the template of the ammonia synthesis plant in Aspen Plus© with some modifications (Fig. 2) (Aspen Technology 2008). The properties of gas and liquid were from the database in Aspen Plus©. The loop scales were 5–1000 tonnes/day. The inlet gas is the stoichiometric ratio of ammonia, i.e., H₂/N₂ = 3.

2.2. Multicatalyst beds and cooling systems

The reaction kinetics of Ru/Ca(NH₂)₂ (Kitano et al., 2018) and Ru/Pr₂O₃ (Imamura et al., 2019) were modeled by the lab-scale experimental data presented in Table 1, showing temperature and pressure ranges. As for pressure, the model was extrapolated based on the available data at low pressure to reproduce the reaction performance at 50 bar since the catalysts are practically expected to be used at 50 bar (Tsubame BHB Co. 2022). The operation temperature in the reactor needs to be elevated to accelerate the reaction, although ammonia synthesis is an exothermic reaction. As the reaction proceeds, the temperature increases to be close to the equilibrium, and the reactivity slows down. Therefore, the reactor needs to cool down when the temperature is too high. The plant generally employs a multi-bed reactor and removes the heat in the outlet of each reactor. The difference between the inlet and outlet (ΔT) was kept <100 K for safety (Woods, 2007). In this study, a three-bed reactor system was applied because it was found to be the most efficient in terms of NH₃ production, energy savings, capital, and maintenance cost (Khademi and Sabbaghi, 2017). The three-bed reactor system consisted of three reactors and two heat exchangers (Fig. 2(b)). If the ammonia concentration is close to equilibrium, the reaction rate slows down and redundantly increases the reactor volume, resulting in a high cost. Hence, a general method was employed to determine the volume, which stops the reaction when the product concentration reaches 90 % of the equilibrium under adiabatic conditions (Nicol et al., 1998). The reaction was stopped when the ΔT increased to = 100 K or when the ammonia concentration in a reactor reached 90 % of the equilibrium, determining the volume of the reactor.

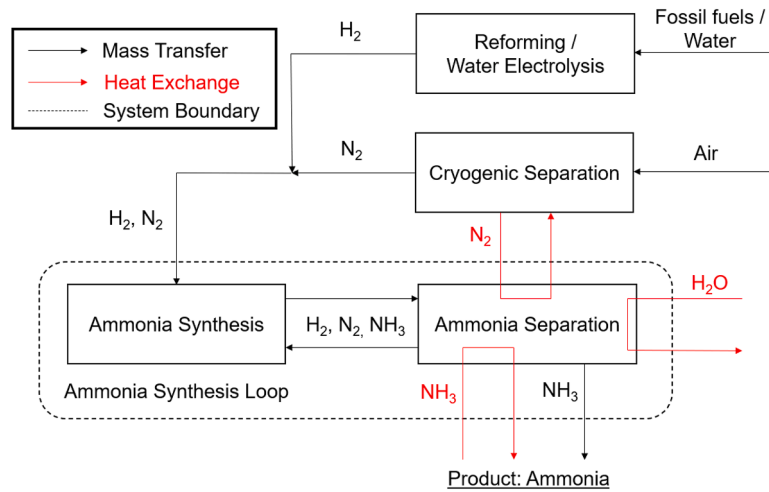


Fig. 1. System boundary of this study. The cost calculation was conducted for the ammonia synthesis loop.

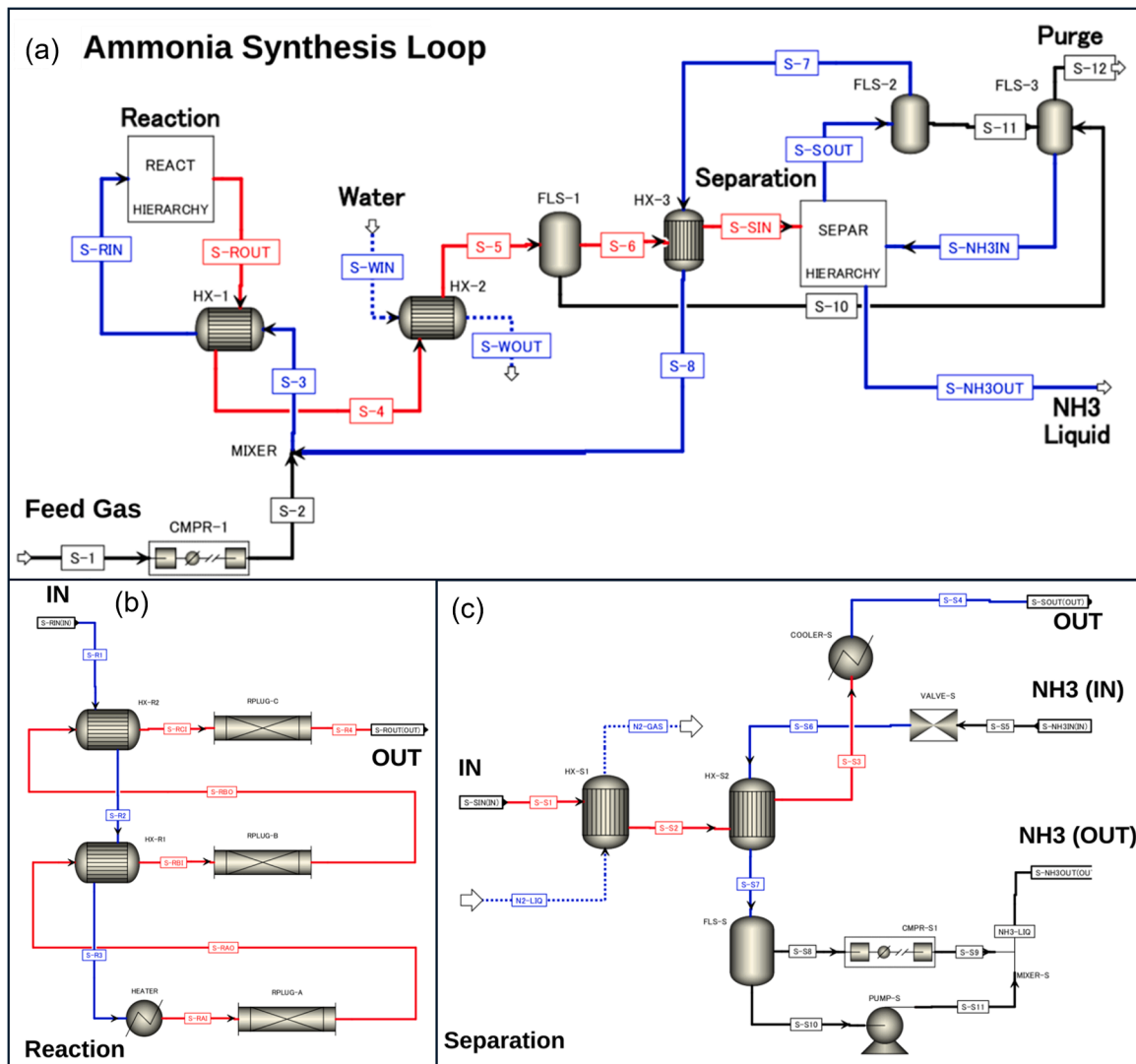


Fig. 2. (a) Overall layout of the ammonia synthesis loop simulation in Aspen Plus© (b) Flowsheet of the ammonia synthesis process; details of the “Reaction” block in the overall flowsheet (c) Flowsheet of the ammonia refrigeration process for the separation of the product NH₃; details of the “Separation” block in the overall flowsheet. The blue- and red-colored streams mean low and high-temperature sides in each heat exchanger, respectively. The black-colored one does not exchange its heat.

Table 1
Reaction conditions utilized for reaction modeling.

Catalyst	Pressure [bar]	Inlet temperature [°C]
KM1R (Fe-based)	150	400–500
Ru/C	100	350–500
Ru/C	50	350–470
Ru/Pr ₂ O ₃	30	300–450
Ru/Ba-Ca(NH ₂) ₂	10	220–360

The reaction temperature ranges for each catalyst were determined by optimization to obtain the lowest cost with the above criteria and available experimental data from the literature (Kitano et al., 2018; Imamura et al., 2019)

2.3. Separation of ammonia by refrigeration

The ammonia concentration at equilibrium is small at high temperature. Thus, plenty of H₂ and N₂ remain unreacted and need to be recycled from the viewpoint of cost. As for recycling, a general method, i.e., refrigeration under high pressure, was employed in ammonia synthesis to produce ammonia liquid and separate the liquid product and the reactant gases. The refrigeration temperature was adjusted to bring the NH₃ molar concentration at the reactor inlet to 3 %, which is the typical value for the ammonia collection in the plant (Liu, 2013). Water was used for initial cooling to room temperature (30 °C), and the cooled nitrogen gas in cryogenic air separation was used in the second step of the cooling. The pressure of the NH₃ product was released, and its latent heat and cold heat were utilized to lower the temperature, followed by the compression of the product to be liquid under 20 bar at room temperature (30 °C) (Fig. 2(c)).

2.4. Kinetics in the reactor

The simple Temkin equation represents plenty of experimental kinetic data for KM1R (Dyson and Simon, 1968; Guacci et al., 1977; Temkin, 1950). However, the Temkin equation cannot describe the experimental kinetic data for Ru-based catalysts well because hydrogen poisoning inhibit the reaction over Ru-based catalysts (Rossetti et al., 2006; Rosowski et al., 1997). Buzzi et al. considered 23 possible kinetic models by the Langmuir–Hinshelwood–Hougen–Watson (LHHW) approach, separating the reaction into elementary reaction steps and expressing the overall reaction as the slowest step rate (Buzzi Ferraris et al., 1974). Rossetti et al. modified the Temkin equation to successfully represent the experimental kinetic data for Ru/C catalyst by the LHHW approach, taking into account hydrogen poisoning (Rossetti et al., 2006). The modified Temkin equation under the condition of the feeding ratio H₂/N₂ = 3 is as follows:

$$r_{\text{NH}_3} = k_f \frac{(a_{\text{N}_2})^n \left[\frac{(a_{\text{H}_2})^{3\alpha}}{(a_{\text{NH}_3})^{2\alpha}} \right]^\alpha - \frac{1}{(K_a)^{2\alpha}} \left[\frac{(a_{\text{NH}_3})^{2\alpha}}{(a_{\text{H}_2})^{3\alpha}} \right]^{1-\alpha}}{1 + K_{\text{H}_2} (a_{\text{H}_2})^{3nw_2} + K_{\text{NH}_3} (a_{\text{NH}_3})^{2nw_3}} \quad (1)$$

where α , w_2 , w_3 , and n are constants, r_{NH_3} is the reaction rate in kmol_{NH₃}/hr/m³ of catalyst beds, k_f is a kinetic constant of the forward reaction, and K_{H_2} and K_{NH_3} are the adsorption equilibrium constants for hydrogen and ammonia, respectively. This equation also includes the influences of reverse reaction (ammonia decomposition) and ammonia poisoning because high a_{NH_3} reduces r_{NH_3} . These parameters of Ru/Ca(NH₂)₂ and Ru/Pr₂O₃ catalysts were modeled by the available experimental data (Kitano et al., 2018; Imamura et al., 2019) through the following equations:

$$k_f = k_0 \exp\left(-\frac{E_a}{RT}\right) \quad (2)$$

$$\log_e K_{\text{H}_2} = -\frac{A_{\text{H}_2}}{R} + \frac{B_{\text{H}_2}}{RT} \quad (3)$$

$$\log_e K_{\text{NH}_3} = -\frac{A_{\text{NH}_3}}{R} + \frac{B_{\text{NH}_3}}{RT} \quad (4)$$

where E_a is the activation energy and A_X and B_X ($X = \text{H}_2$ or NH_3) are the constants. E_a s of the catalysts are referred to experimental data (Kitano et al., 2018; Imamura et al., 2019). The equilibrium constant K_a was calculated according to Gillespie and Beattie: (Dyson and Simon, 1968; Rossetti et al., 2006; Gillespie and Beattie, 1930)

$$\log_{10} K_a = -2.691122 \log_{10} T - 5.519265 \times 10^{-5} T + 1.848863 \times 10^{-7} T^2 + \frac{2001.6}{T} + 2.6899 \quad (5)$$

For gas, the activity of a component can be expressed as follows:

$$a_i = \frac{f_i}{P^\ominus} \quad (6)$$

where f_i is the fugacity of the component i and P^\ominus is the standard pressure. Choosing P^\ominus as equal to 1 atm, one can be written as

$$a_i = f_i = \varphi_i y_i P \quad (7)$$

where φ_i is the fugacity coefficient of component i , y_i is the molar fraction of component i , and P is the pressure in atm. We employed the fugacity coefficients calculated by Cooper and Shaw et al. for hydrogen and by Cooper and Newton for nitrogen and ammonia (Dyson and Simon, 1968; Rossetti et al., 2006; Shaw and Wones, 1964; Newton, 1935)

$$\varphi_{\text{H}_2} = \exp\left\{ \exp(-3.8402T^{0.125} + 0.541)P - \exp(-0.1263T^{0.5} - 15.980)P^2 + 300[\exp(-0.011901T - 5.941)] \left[\exp\left(-\frac{P}{300}\right) \right] \right\} \quad (8)$$

$$\varphi_{\text{N}_2} = 0.93431737 + 0.3101804 \times 10^{-3}T + 0.295896 \times 10^{-3}P - 0.2707279 \times 10^{-6}T^2 + 0.4775207 \times 10^{-6}P^2 \quad (9)$$

$$\varphi_{\text{NH}_3} = 0.1438996 + 0.2028538 \times 10^{-2}T - 0.4487672 \times 10^{-3}P - 0.1142945 \times 10^{-5}T^2 + 0.2761216 \times 10^{-6}P^2 \quad (10)$$

The nine constants in the above equations, i.e., k_0 , α , w_2 , w_3 , n , A_{H_2} , A_{NH_3} , B_{H_2} , and B_{NH_3} , are determined by the least squares method with the following optimization methods:

Step 1. Temporally substituting the initial parameter values in the equations.

Step 2. Simulating the reaction using the current parameters in the repeated steps. The instantaneous reaction rate is derived from Eq (1). The reaction proceeds according to the obtained reaction rate, and the isothermal and isobaric gas ratios of N₂, H₂, and NH₃ are updated. One reaction step was assumed to be 1 msec. The reaction rate is recalculated by Eq. (1) based on the updated gas composition. These are repeated until the total reaction time reaches the estimated residence time. The obtained ammonia concentrations $C_{\text{NH}_3}^{\text{out}}$ [%] are compared with the experimental results.

Step 3. Updating the nine constants to minimize the squares of errors between the simulation and experimental results of $C_{\text{NH}_3}^{\text{out}}$ each experiment. Return to step 2.

Step 4. Obtaining the final parameters when the difference in the cycle is lower than 10^{-8} .

Trust region reflective algorithm was utilized to determine the

parameters in the least squares method (Yuying, 1993). The obtained reaction kinetics were implemented using Fortran subroutines of the plug flow reactor (RPlug) model in Aspen Plus®, and the “RPlug” model was adopted in adiabatic conditions. The kinetics for KM1R and R/C were the same as those in our previous report (Yoshida et al., 2021)

2.5. Economic analysis

The total cost for the loops is separated into a capital cost, C^{cap} , and an operation cost, C^{op} . C^{cap} was estimated by using the following equations: (Woods, 2007)

$$C^{cap} = \sum_j C_j \quad (11)$$

$$C_j = \left(C_{j,fix} + LM \times AF \times C_{j,ref} \times \left(\frac{s_j}{s_{ref}} \right)^{n_j} \right) \times \frac{CEPCI}{1000} \quad (12)$$

where C_j is the bare module cost for equipment j , $C_{j,fix}$ is the cost of the control system of j , LM is the cost of labor and materials, AF is an alloy factor that is determined by the cost of materials, $C_{j,ref}$ is the cost for j in a reference scale s_{ref} , s_j is the actual scale of j , and n_j is a parameter that determines the influence of a scale. Table 2 presents the parameters in Eq. (12) for each piece of equipment, j , assuming that the chemical plant cost index (CEPCI) is 1000. In the plant embedded with Ru/Ca(NH₂)₂ at 10 bar, the required temperature for cooling was too low, -51.9 °C, which is lower than the boiling point of refrigerant, ammonia (-33.3 °C). Mechanical vapor recompression (refrigerator) was then employed in the refrigeration process, referring to the literature (Woods, 2007). The adjustment factor in Table 3 is multiplied to the $C_{j,ref}$ ($j =$ reactor or refrigerator) on a reference scale. Stainless steel (SUS 304) was employed as the material for reactors, compressors, and heat exchangers (shell and tube) with an alloy factor of 2.75 for reactors and compressors and 2.80 for heat exchangers (Woods, 2007). This is because SUS 304 is durable for the temperature and pressure required for the plants and is tolerant to hydrogen embrittlement (Ashby, 2009; Committee of Stainless Steel Producer 1978). A CEPCI of 607.5 was utilized in 2019 (before the COVID-19 pandemic).

C^{op} was calculated using the following equation: (Woods, 2007)

$$C^{op} = \sum_{t=1}^{year} \frac{1}{(1+d)^{t-1}} (P_{elec} E_{year} + P_{cat}(duration, t) \times BD \times V_{reactor}) \quad (13)$$

$$P_{cat}(duration, t) = \begin{cases} p_{cat}(duration = 1) \\ p_{cat}(duration > 1, t \equiv 1(mod\ duration)) \\ 0 (duration > 1, t \not\equiv 1(mod\ duration)) \end{cases} \quad (14)$$

where $year$, i.e., the duration of the operation, is assumed as 20 years. Assuming that the plant was implemented in the USA due to the available data, d is the discount rate, accounting to 2.25 % (data in 2019, before the COVID-19 pandemic) (Fund, 2023) P_{elec} is the cost for electricity, and two patterns are assumed, i.e., 0.0683 USD/kWh, which is the price for the industrial sector in the USA in 2019, (U.S. Energy Information Administration 2020) and 0.273 USD/kWh, which is the price for photovoltaics with rechargeable batteries (batteries 0.206 \$/kWh +

Table 2
Summary of the parameters for Eq. (14) (Woods, 2007).

Unit	Basis	$C_{j,fix}$	$C_{j,ref}$	s_{ref}	n_j	LM	AF
Reactor	Volume [m ³]	63,000	110,000	20	0.52	2.30	2.75
Compressor, low	Rated power [kW]	7000	1350,000	1000	0.90	2.15	2.75
Compressor, high	Rated power [kW]	7000	10,300,000	10,000	0.71	2.15	2.75
Heat exchanger	Area [m ²]	27,000	70,000	100	0.71	2.80	2.80
Pump, small	Rated power [kW]	7000	7000	16	0.26	1.47	1.90
Pump, large	Rated power [kW]	7000	7000	16	0.43	1.47	1.90
Refrigerator	Rated power [kW]	40,000	800,000	1000	0.77	1.30	1.00

Table 3
Adjustment factors for the reactor and refrigerator.

Equipment	Unit	Values	Adjustment Factor
Reactor	bar	150	3.4
	bar	100	2.3
	bar	75	1.9
	bar	50	1.6
	bar	30	1.3
	bar	10	1.0
Refrigerator	°C	-40	4.0
	°C	-51	7.0

Table 4
Price, bulk density, and porosity of the catalysts.

Catalyst	Ru content [wt%]	Price [USD/g]	Bulk density [g/cm ³]	Porosity [-]
KM1R	-	0.020	2.80	0.52
Ru/C	3.2	0.608	0.80	0.63
Ru/Pr ₂ O ₃	5	0.950	2.59	0.60
Ru/Ba-Ca(NH ₂) ₂	10	1.900	0.79	0.60

photovoltaics 0.067 \$/kWh) under US circumstance (Comello and Reichelstein, 2019). The required energy per year, E_{year} , is estimated by the output from Aspen Plus®.

The term “ $P_{cat}(duration, t) \times BD \times V_{reactor}$ ” calculates the catalyst cost used in the plant. The catalyst cost is generally estimated by weight and material cost per weight without the economy of scale (Peters et al., 2003) $P_{cat}(duration, t)$ is the catalyst price [USD/kg] and is determined for each year by Eq (14). $P_{cat}(duration, t)$ depends on the catalyst durability period ($duration$), and the cost is incurred when the catalyst is replaced. The influence of $duration$ was evaluated by changing it from 1 to 10 years. BD is the bulk density of the catalyst used [g/cm³], and $V_{reactor}$ is the volume of the reactor used in the ammonia synthesis loop [m³]. Table 4 summarizes the catalyst prices, bulk densities, and porosity of the four catalysts used in this study. BD of KM1R (iron-based catalyst) (Dyson and Simon, 1968) and Ru/C (Rossetti and Forni, 2005) was obtained from literature values, while BD of the recent catalysts (Ru/Pr₂O₃ and Ru/Ba-Ca(NH₂)₂) was calculated to obtain a porosity of 0.60 when the catalyst was packed in the reactor (Liu, 2013; Dyson and Simon, 1968). The price of KM1R (iron-based catalyst) was set at 0.02 USD/g based on past transactions (Zauba 2022). The cost of ruthenium-based catalyst, p_{cat} , was calculated by multiplying the amount of ruthenium contained in the catalyst by the unit price of ruthenium (19 USD/g) (Umicore 2024) Ru/Ca(NH₂)₂ and Ru/Pr₂O₃ have 10 and 5 wt% of Ru, respectively (Kitano et al., 2018; Imamura et al., 2019)

3. Results

3.1. Validation of simulated results

These fitting results based on Section 2.4 are shown here, different from the results using Aspen Plus®. Table 5 presents the parameter values obtained through the least squares method. Figs. 3 and 4 show the

Table 5

Parameter values obtained through the least squares method. The values for KM1R and Ru/C were the same as those in our previous report (Yoshida et al., 2021).

Catalyst	E_a [kJ mol ⁻¹]	k_0	n	α	w_2	w_3	A_{H_2}	B_{H_2}	A_{NH_3}	B_{NH_3}
Ru/Pr ₂ O ₃	101	1.13×10^{10}	0.21	0.10	0.10	0.10	15.4	509	17.7	424.0
Ru/Ba-Ca(NH ₂) ₂	59.4	8.64×10^6	0.73	0.10	0.18	0.10	5.9	8742	96.4	5073

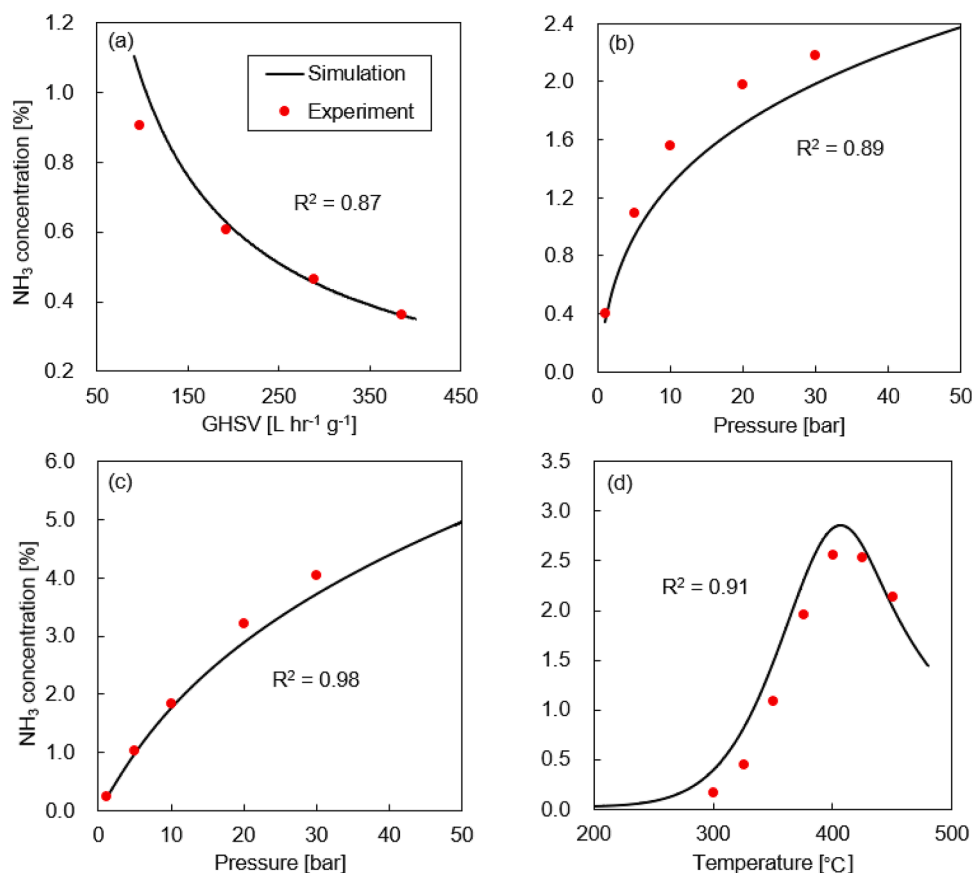


Fig. 3. Experimental and simulated $C_{NH_3}^{out}$ of Ru/Pr₂O₃ against (a) gas hourly space velocity (GHSV) at 400 °C and 10 bar, (b) pressure at 400 °C and 72 L h⁻¹ g⁻¹, (c) pressure at 450 °C and 72 L h⁻¹ g⁻¹, and (d) temperature at 10 bar and 18 L h⁻¹ g⁻¹.

$C_{NH_3}^{out}$ of experiments using Ru/Pr₂O₃ and Ru/Ba-Ca(NH₂)₂ and simulation results of a single pass over the reactor for validation based on the values presented in Table 5. In the case of Ru/Pr₂O₃, the simulation results approximately describe the experimental values, although the error tends to be significant at higher pressure conditions. As for Ru/Ba-Ca(NH₂)₂, the R² values of the fitting are high, and the modeling is sufficiently accurate at various reaction conditions. Thus, it was found that the modified Temkin model reproduces the experimental results for each of the new Ru-based catalysts, i.e., Ru/Pr₂O₃ and Ru/Ba-Ca(NH₂)₂, by parameter fitting through the least squares method. It is the first example of modeling the reactions of Ru-based catalysts other than Ru/C with the modified Temkin equation, which considers the reverse reaction.

Fig. 5 shows the $C_{NH_3}^{out}$ of Ru/Pr₂O₃ and Ru/Ba-Ca(NH₂)₂ at 10–50 bar, predicted by the extrapolation of the results under low pressures. The $C_{NH_3}^{out}$ reaches its peak at 350–450 °C, and the peak temperature increases at higher pressure. The equilibrium concentration of ammonia is reduced at higher temperatures and increases at larger pressures. In addition, Figs. 3(d), 4(a), and (b) showed the peaks against temperature. The reaction rates in these figures are then influenced by the chemical equilibrium in the high-temperature region. These reflect the reverse reaction in Eq. (1).

3.2. Overall cost of the ammonia synthesis loop under low pressures with industrial electricity

First, to show simulation results without extrapolations, the total cost was evaluated at pressures of 30 bar and 10 bar for Ru/Pr₂O₃ and Ru/Ba-Ca(NH₂)₂, respectively, which are pressures near the available experimental data. An amount of 0.0683 USD/kWh was utilized for the electricity cost. Fig. 6 shows the total costs and their breakdown. The operating conditions for each catalyst and pressure were optimized to achieve the lowest total cost. As shown in Fig. 6, the catalyst is the most expensive, even with a 10-year catalyst durability. This is because the reported reaction rates under mild conditions are not fast enough, and the reactor volume and the amount of catalyst required to fill it are too large. Under these conditions, the larger amount of Ru is critical to the cost; Ru/Ba-Ca(NH₂)₂ is more costly than Ru/Pr₂O₃ because of its twice Ru weight. Considering the industrialization of ammonia synthesis catalysts, the reaction conditions published in the paper base should be closer to the industrial process.

At a plant scale of 100 tonnes/day, the ratio of the power cost to the total cost is more significant than that of the equipment cost. Due to economies of scale in equipment costs, the percentage of equipment costs to the total expenses decreases further if the plant scale is larger than 100 tonnes/day and vice versa in the case of a plant scale smaller

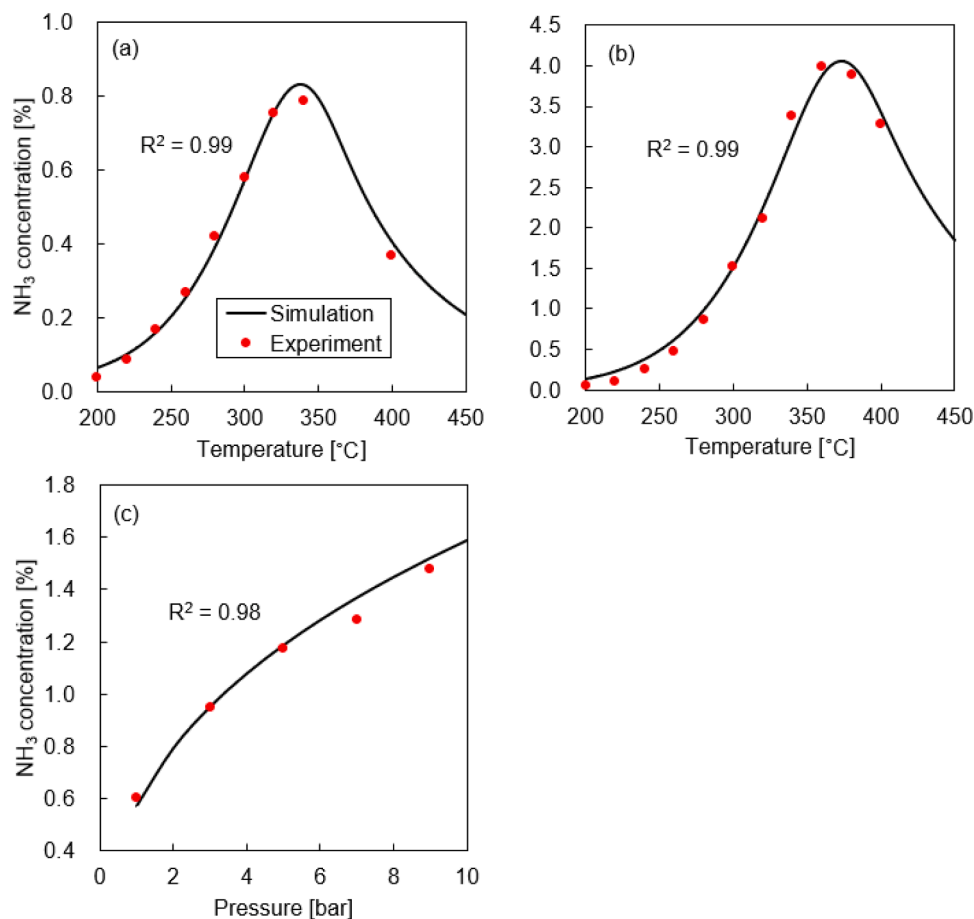


Fig. 4. Experimental and simulated $C_{NH_3}^{out}$ of Ru/Ba-Ca(NH₂)₂ against (a) temperature at 1 bar and 36 L h⁻¹ g⁻¹, (b) temperature at 9 bar and 36 L h⁻¹ g⁻¹, and (c) pressure at 300 °C and 36 L h⁻¹ g⁻¹.

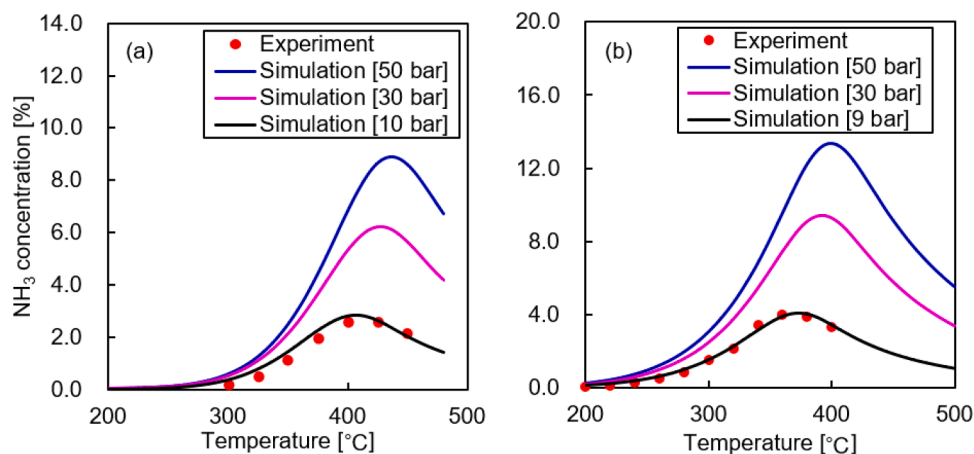


Fig. 5. Extrapolated $C_{NH_3}^{out}$ until 50 bar over Ru/Pr₂O₃ (18 L h⁻¹ g⁻¹) and Ru/Ba-Ca(NH₂)₂ (36 L h⁻¹ g⁻¹).

than 100 tonnes/day.

In addition, Ru/Pr₂O₃ and Ru/Ba-Ca(NH₂)₂ save electricity for the compression of the introduced gas due to their low pressure. On the other hand, the low pressure makes liquefaction and recovery difficult, and as presented in Table 6, very low temperatures are required. In other words, the advantage of reduced power costs due to lower pressure reaction conditions is offset by the power necessary at lower temperatures in the recovery process. This conclusion is consistent with our previous report (Yoshida et al., 2021)

3.3. Overall cost of the ammonia synthesis loop under high pressures with industrial electricity

As shown in Section 3.2, the experimental data reported in the literature are unsuitable for practical use. The extrapolated data of the reaction rate under 50 bar are then utilized for comparison. An amount of 0.0683 USD/kWh was used for the electricity cost. Fig. 7 shows the breakdown of the total cost for the ammonia synthesis loop at a scale of 100 tonnes/day. The high pressure significantly improved the reaction

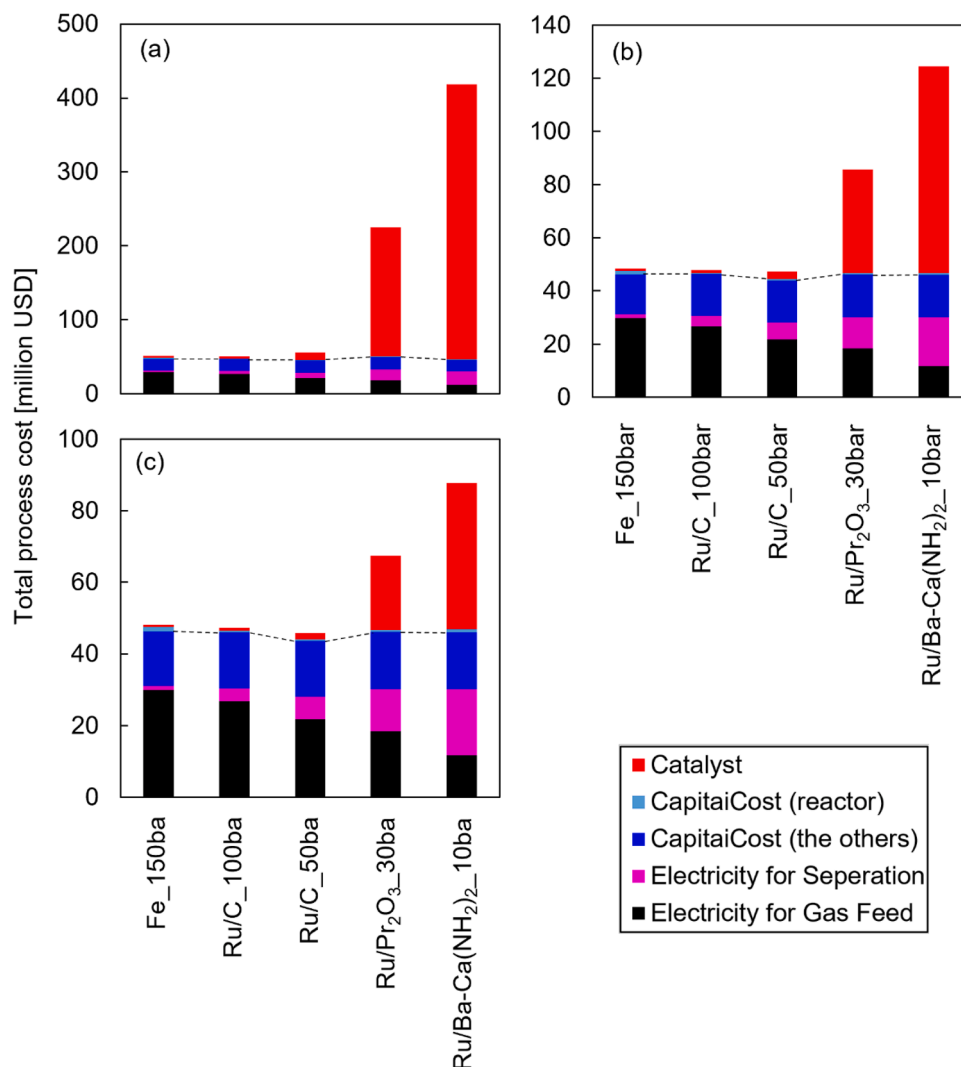


Fig. 6. Breakdown of the cost for the ammonia synthesis loop under low pressure for Ru/Pr₂O₃ and Ru/Ba-Ca(NH₂)₂ at a scale of 100 tonnes/day ($P_{elec} = 0.0683$ USD/kWh) in the duration of the catalyst: (a) 1, (b) 5, and (c) 10 years. The dotted line shows the border of the cost related to catalysts (Catalyst & Capital cost (reactor)) and the others.

Table 6

Separation temperature for each process.

Catalyst	Pressure [bar]	Separation temperature [°C]
KM1R (Fe-based)	150	-3.3
Ru/C	100	-10.1
Ru/C	50	-24.5
Ru/Pr ₂ O ₃	30	-32.9
Ru/Ba-Ca(NH ₂) ₂	10	-51.9
Ru/Pr ₂ O ₃	50 (extrapolation)	-23.3
Ru/Ba-Ca(NH ₂) ₂	50 (extrapolation)	-21.2

rate of Ru/Ba-Ca(NH₂)₂. Under the conditions with elevated pressure, the higher activity of Ru/Ba-Ca(NH₂)₂ is more beneficial than that of Ru/Pr₂O₃ despite the twice Ru amount. Besides, the separation temperatures of the new catalysts are comparable with conventional ones, as shown in Table 6 below, resulting in reduced costs for the total electricity. If the duration of Ru/Pr₂O₃ and Ru/Ba-Ca(NH₂)₂ is 10 years, the total cost is equivalent with that of conventional catalysts. However, the advantages of new catalysts for the whole cost are not evident in these conditions.

3.4. Overall cost of the ammonia synthesis loop under high pressures with photovoltaics and rechargeable batteries

With the extrapolated data under 50 bar, it was assumed that renewable energy is utilized to produce ammonia at a small scale locally: the production scale is 5 tonnes/day, and the electricity cost is 0.273 USD/kWh bearing photovoltaics and rechargeable battery. Fig. 8 shows the breakdown of the total cost for the ammonia synthesis loop under these assumptions. If the duration of the new catalysts is 10 years, the total cost of Ru/Ba-Ca(NH₂)₂ is lower than that of conventional catalysts. Therefore, the new catalysts are advantageous if the high electricity cost, the small production scale, and the long catalyst duration. The former two points are the characteristics of green ammonia synthesis; thus, the new catalysts are suitable for green ammonia production.

The electricity price changes depending on the cost of photovoltaics and rechargeable batteries. To investigate the "break-even" points of these catalysts, we plotted the total process cost using these catalysts against the electricity price in Fig. 9. The ammonia synthesis loop is under high pressure for Ru/Pr₂O₃ and Ru/Ba-Ca(NH₂)₂ at a scale of 5 tonnes/day in the duration of the catalyst of 10 years. Ru/Ba-Ca(NH₂)₂ and Ru/C at 50 bar shows the best performance in the range of 0.07–0.27 USD/kWh. In the higher range than 0.10 USD/kWh, Ru/Ba-

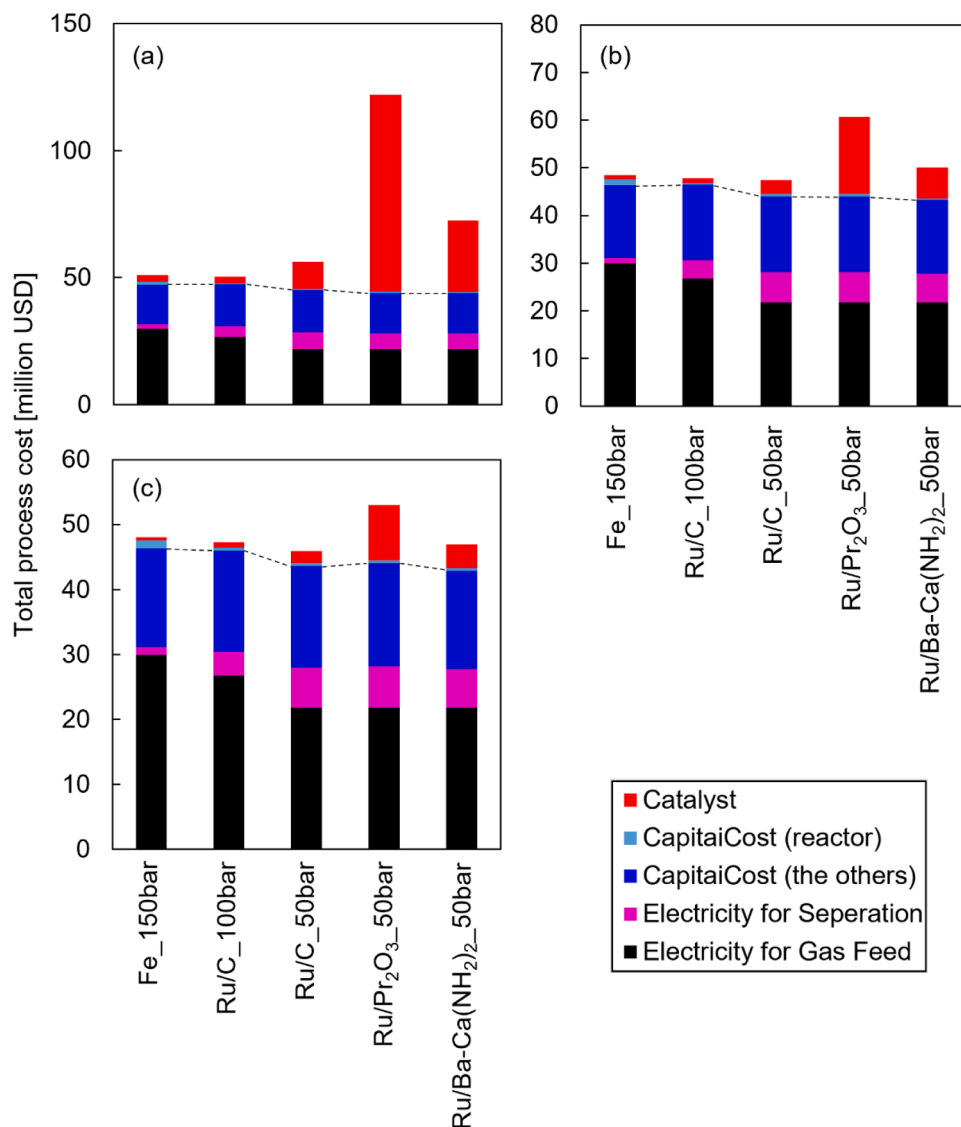


Fig. 7. Breakdown of the cost for the ammonia synthesis loop under high pressure for Ru/Pr₂O₃ and Ru/Ba-Ca(NH₂)₂ at a scale of 100 tonnes/day ($P_{elec} = 0.0683$ USD/kWh) in the duration of the catalyst: (a) 1, (b) 5, and (c) 10 years. The dotted line shows the border of the cost related to catalysts (Catalyst & Capital cost (reactor)) and the others.

Ca(NH₂)₂ at 50 bar demonstrates the lowest cost among these catalysts.

4. Discussion

Based on the results of total costs, the high activity of the new catalysts reduces the electricity cost for pressurizing reactant gases; however, the electricity for lowering the temperature in ammonia separation through liquefaction is significant due to the mitigated pressure and almost compensates for the decreased cost. The dotted lines in Figs. 6, 7, and 8 show the sum of the costs unrelated to the catalyst performance. This means the minimum cost at a specific temperature and pressure when the catalytic activity is ideally high: the amount of catalyst and the reactor volume is small, giving negligible cost related to the catalyst. Figs. 7 and 8 show that the newly developed catalysts are slightly advantageous when the high electricity price. Moreover, the dotted line in Fig. 6 indicates the total minimum cost is not so different, even if the ideal catalyst demonstrates high performance at lower pressure. This conclusion is consistent with our previous report that analyzed Ru/C, (Yoshida et al., 2021) despite the significantly enhanced activity of new catalysts. These results show the economic limitation of the current research trends that develop a catalyst for ammonia synthesis under low

pressure. Mitigating reaction pressure might not be meaningful from the viewpoint of economics in traditional circumstances. Low operation temperature is still beneficial because it is preferable to obtain ammonia in terms of chemical equilibrium, although waste heat of the ammonia synthesis readily increases the temperature without energy loss and reducing temperature does not omit the heat.

Nevertheless, as mentioned in the introduction, ammonia synthesis under a mild reaction condition is required to utilize renewable energy due to its time variability. In addition, the new catalysts are economically advantageous when the electricity cost is high, which is the characteristic of the case in which renewable energy is employed. The electricity price is dominant on a large scale, and the capital cost is dominant, based on the results in our previous publication (Yoshida et al., 2021). This tendency is the same as that of this research because only capital costs have economies of scale. Therefore, the small scale is not preferable for renewable energy usage. However, despite the small scale of 5 tonnes/day, the new catalysts have high performance. Fig. 9 indicates a relatively larger range, >0.10 USD/kWh, Ru/Ba-Ca(NH₂)₂ at 50 bar demonstrates the lowest cost among these catalysts. It means that the newly developed catalysts are appropriate for green ammonia synthesis. However, the advantage was proposed with the assumption of the

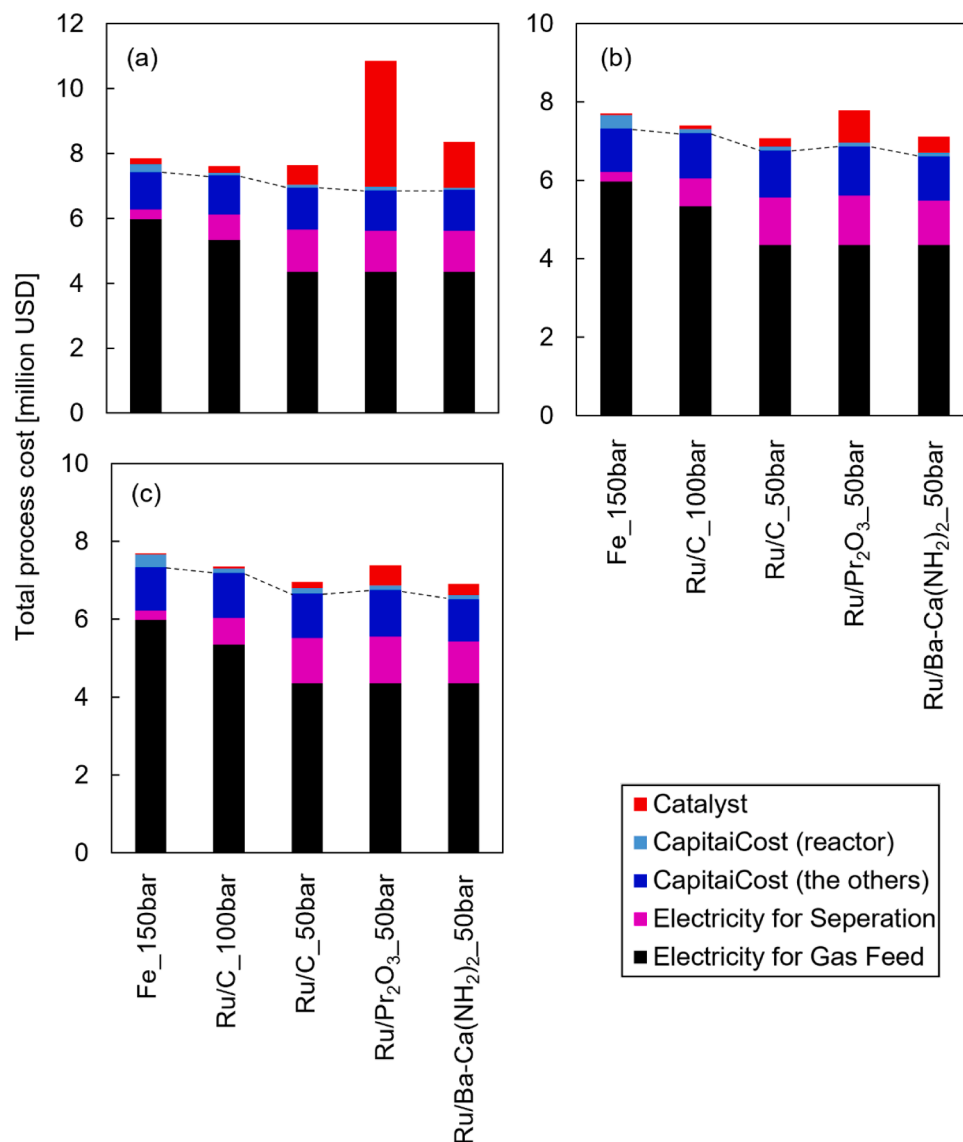


Fig. 8. Breakdown of the cost for the ammonia synthesis loop under high pressure for Ru/Pr₂O₃ and Ru/Ba-Ca(NH₂)₂ at a scale of 5 tonnes/day ($P_{elec} = 0.273$ USD/kWh) in the duration of the catalyst: (a) 1, (b) 5, and (c) 10 years. The dotted line shows the border of the cost related to catalysts (Catalyst & Capital cost (reactor)) and the others.

long durability of the catalysts, such as ten years.

It is noted that catalyst costs are high due to expensive ruthenium; thus, the lifetime of catalysts significantly influences the total cost. This study did not consider recycling or reactivating the catalysts, while these processes have almost the same role with a longer lifetime of the catalysts on the cost calculation. Therefore, the investigation of these processes and extending their lifetime will be critical. On the other hand, the catalytic activity is more emphasized than the Ru amount by the comparison of Ru/Ca(NH₂)₂ and Ru/Pr₂O₃. Focusing on catalytic activity per Ru weight will be meaningful rather than decreasing the amount of Ru. Otherwise, the catalysts bearing cheap metal, such as Ni (Ye et al., 2020; Wang et al., 2017; Gao et al., 2019; Humphreys et al., 2018; Bion et al., 2015; Kojima and Aika, 2001) or Co (Sato et al., 2021; Inoue et al., 2019; Hagen et al., 2002; Rarogpilecka et al., 2006; Lin et al., 2014; Zybert et al., 2022; Ronduda et al., 2021), effectively reduce the catalyst costs. However, as mentioned above with the dotted lines in Figs. 6–8, the ideal catalyst does not reduce the total cost significantly, even if cheap metals are employed.

The advantage of low-pressure processes achieved by the new catalysts is insignificant in electricity consumption because the low pressure

increases the power required to cool and separate the synthesized ammonia as liquid. Instead of cooling separation, the methods based on adsorbents, such as alkali metal salts, which selectively and reversibly absorb ammonia, are promising (Wagner et al., 2017; Malmali et al., 2018). Since the absorption of ammonia occurs at around 200 °C, the synthesized gas does not need to be cooled to the temperature at which ammonia condenses, which will reduce the cost of compressors, heat exchangers, and electricity. The alternative method will eliminate the cost compensation by liquefaction under low pressure and give a vital meaning to the condition mitigated by the newly developed catalysts in terms of economy. Otherwise, electrochemical synthesis of ammonia is hopeful because this method makes it possible to overcome chemical equilibrium and give a high concentration of ammonia in effluent at a practical time scale, which is advantageous in ammonia collection.

5. Conclusions

We evaluated the cost of the ammonia synthesis loops embedded with Ru/Ca(NH₂)₂ and Ru/Pr₂O₃, which are newly developed and very active catalysts under mild conditions. The condition mitigated by the

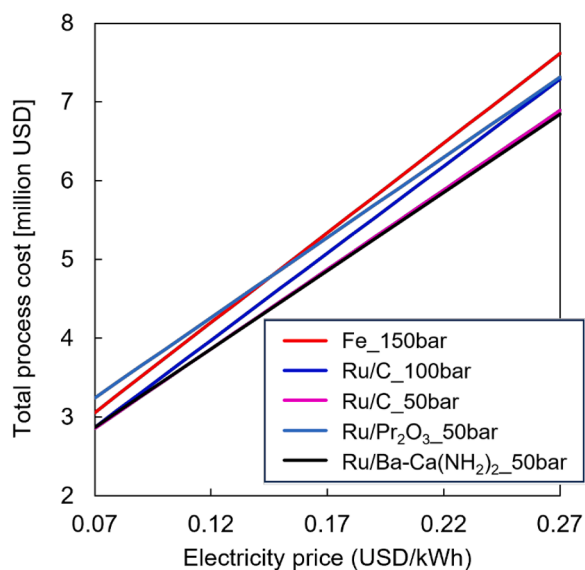


Fig. 9. The total process cost for the ammonia synthesis loop under high pressure for Ru/Pr₂O₃ and Ru/Ba-Ca(NH₂)₂ at a scale of 5 tonnes/day in the duration of the catalyst of 10 years.

new catalysts reduces the electricity cost for pressurizing reactant gases but increases the electricity for ammonia separation through liquefaction due to the mitigated pressure, almost compensating for the decreased cost. The results showed that the cost for ruthenium is dominant, and the lifetime of catalysts is one of the critical parameters. Moreover, the new catalysts are advantageous for green ammonia synthesis in the case that the electricity price is high. Finally, as the directions for further research, the results suggest reducing catalyst costs, such as extending the catalyst lifetime, recycling or reactivating the catalysts, substituting ruthenium with cheap metal, and especially alternative methods to collect ammonia.

CRedit authorship contribution statement

Masaki Yoshida: Data curation, Investigation, Methodology, Validation, Visualization. **Takaya Ogawa:** Conceptualization, Data curation, Formal analysis, Funding acquisition, Investigation, Methodology, Project administration, Resources, Software, Supervision, Validation, Visualization, Writing – original draft, Writing – review & editing. **Keiichi N. Ishihara:** Validation.

Declaration of competing interest

The authors declare that they have no known competing financial interests or personal relationships that could have appeared to influence the work reported in this paper.

Data availability

Data will be made available on request.

Acknowledgment

This research was supported by the Environment Research and Technology Development Fund (JPMEERF20192R02) of the Environmental Restoration and Conservation Agency of Japan and partially Japan Science and Technology Agency (JST), Precursory Research for Embryonic Science and Technology (PRESTO). Grant Number JPMJPR2273, Japan.

References

- Aika, K., Ozaki, A., Hori, H., 1972. acTivation of nitrogen by alkali-metal promoted transition-metal .1. Ammonia synthesis over ruthenium promoted by alkali-metal. *J. Catal.* 27 (3), 424–431.
- Aika, K.I., 2017. Role of alkali promoter in ammonia synthesis over ruthenium catalysts—effect on reaction mechanism. *Catal. Today* 286, 14–20.
- Al-Zareer, M., Dincer, I., Rosen, M.A., 2018. Transient analysis and evaluation of a novel pressurized multistage ammonia production system for hydrogen storage purposes. *J. Clean. Prod.* 196, 390–399.
- Anderson, J.S., Rittle, J., Peters, J.C., 2013. Catalytic conversion of nitrogen to ammonia by an iron model complex. *Nature* 501 (7465), 84–.
- Andersson, J., Lundgren, J., 2014. Techno-economic analysis of ammonia production via integrated biomass gasification. *Appl. Energy* 130, 484–490.
- Araújo, A., Skogestad, S., 2008. Control structure design for the ammonia synthesis process. *Comput. Chem. Eng.* 32 (12), 2920–2932.
- Arashiba, K., Miyake, Y., Nishibayashi, Y., 2011. A molybdenum complex bearing PNP-type pincer ligands leads to the catalytic reduction of dinitrogen into ammonia. *Nat. Chem.* 3 (2), 120–125. Article.
- Arora, P., Hoadley, A.F.A., Mahajani, S.M., Ganesh, A., 2016. Small-scale ammonia production from biomass: a techno-enviro-economic perspective. *Ind. Eng. Chem. Res.* 55 (22), 6422–6434.
- Ashby, M. *Material and process charts.* 2009, (Chart 12).
- Ashida, Y., Arashiba, K., Nakajima, K., Nishibayashi, Y., 2019. Molybdenum-catalysed ammonia production with samarium diiodide and alcohols or water. *Nature* 568 (7753), 536–540.
- Aspen Technology, I. *Aspen Plus Ammonia Model.* 2008.
- Atkins, P.W.; De Paula, J.; Keeler, J. *Atkins' Physical Chemistry;* Oxford University Press, 2018.
- Bicer, Y., Dincer, I., Zamfirescu, C., Vezina, G., Raso, F., 2016. Comparative life cycle assessment of various ammonia production methods. *J. Clean. Prod.* 135, 1379–1395.
- Bion, N., Can, F., Cook, J., Hargreaves, J.S.J., Hector, A.L., Levason, W., McFarlane, A.R., Richard, M., Sardar, K., 2015. The role of preparation route upon the ambient pressure ammonia synthesis activity of Ni₂Mo₃N. *Appl. Catal. A-Gen* 504, 44–50.
- Brown, D.E., Edmonds, T., Joyner, R.W., McCarroll, J.J., Tennison, S.R., 2014. The genesis and development of the commercial bp doubly promoted catalyst for ammonia synthesis. *Catal. Lett.* 144 (4), 545–552.
- Buzzi Ferraris, G., Donati, G., Rejna, F., Carrà, S., 1974. An investigation on kinetic models for ammonia synthesis. *Chem. Eng. Sci.* 29 (7), 1621–1627.
- Chalkley, M.J., Drover, M.W., Peters, J.C., 2020. Catalytic N₂-to-NH₃ (or -N₂H₄) conversion by well-defined molecular coordination complexes. *Chem. Rev.* 120 (12), 5582–5636.
- Chauhan, M., 2018. Africa fertilizer market outlook: challenges and Opportunities for GCC pricedures. *Nexant* 1–14.
- Comello, S., Reichelstein, S., 2019. The emergence of cost effective battery storage. *Nat. Commun.* 10 (1), 2038.
- Committee of Stainless Steel Producer, A. I. a. S. I. *Stainless Steel in Ammonia Production.* 1978.
- Donald, G.; Robert. H. Start-up method for ammonia plants. U. S. Patent US-4728506-A, March 1, 1986.
- Dyson, D.C., Simon, J.M., 1968. Kinetic expression with diffusion correction for ammonia synthesis on industrial catalyst. *Ind. Eng. Chem. Fundam.* 7 (4), 605–610.
- Fraattini, D., Cinti, G., Bidini, G., Desideri, U., Cioffi, R., Jannelli, E., 2016. A system approach in energy evaluation of different renewable energies sources integration in ammonia production plants. *Renew. Energy* 99, 472–482.
- Fund, I.M. Interest rates, discount rate for united states. <https://fred.stlouisfed.org/series/INTDSRUSM193N> (accessed 2023 January 14th).
- Götz, M., Lefebvre, J., Mörs, F., McDaniel Koch, A., Graf, F., Bajohr, S., Reimert, R., Kolb, T., 2016. Renewable power-to-gas: a technological and economic review. *Renew. Energy* 85, 1371–1390.
- Gao, W., Guo, J., Chen, P., 2019. Hydrides, amides and imides mediated ammonia synthesis and decomposition. *Chin. J. Chem.* 37 (5), 442–451.
- Gillespie, L.J., Beattie, J.A., 1930. The thermodynamic treatment of chemical equilibria in systems composed of real gases. I. An approximate equation for the mass action function applied to the existing data on the haber equilibrium. *Phys. Rev.* 36 (4), 743–753.
- Guacci, U., Traina, F., Ferraris, G.B., Barisone, R., 1977. On the application of the Temkin equation in the evaluation of catalysts for the ammonia synthesis. *Ind. Eng. Chem. Process Des. Dev.* 16 (2), 166–176.
- Hagen, S., Barfod, R., Fehrmann, R., Jacobsen, C.J., Teunissen, H.T., Stahl, K., 2002. Chorkendorff, I. New efficient catalyst for ammonia synthesis: barium-promoted cobalt on carbon. *Chem. Commun.* (11), 1206–1207.
- Hasan, A., Dincer, I., 2019. Development of an integrated wind and PV system for ammonia and power production for a sustainable community. *J. Clean. Prod.* 231, 1515–1525.
- Hattori, M., Mori, T., Arai, T., Inoue, Y., Sasase, M., Tada, T., Kitano, M., Yokoyama, T., Hara, M., Hosono, H., 2018. Enhanced catalytic ammonia synthesis with transformed BaO. *ACS Catal.* 10977–10984.
- Humphreys, J., Lan, R., Du, D., Xu, W., Tao, S., 2018. Promotion effect of proton-conducting oxide BaZr_{0.1}Ce_{0.7}Y_{0.2}O_{3-δ} on the catalytic activity of Ni towards ammonia synthesis from hydrogen and nitrogen. *Int. J. Hydrog. Energy* 43 (37), 17726–17736.
- Imamura, K., Miyahara, S.I., Kawano, Y., Sato, K., Nakasaka, Y., Nagaoka, K., 2019. Kinetics of ammonia synthesis over Ru/Pr₂O₃. *J. Taiwan Inst. Chem. Eng.* 105, 50–56.

- Inoue, Y., Kitano, M., Tokunari, M., Taniguchi, T., Ooya, K., Abe, H., Niwa, Y., Sasase, M., Hara, M., Hosono, H., 2019. Direct activation of cobalt catalyst by $12\text{CaO}\cdot 7\text{Al}_2\text{O}_3$ electride for ammonia synthesis. *ACS Catal.* 9 (3), 1670–1679.
- Khademi, M.H., Sabbaghi, R.S., 2017. Comparison between three types of ammonia synthesis reactor configurations in terms of cooling methods. *Chem. Eng. Res. Des.* 128, 306–317.
- Kitano, M., Inoue, Y., Yamazaki, Y., Hayashi, F., Kanbara, S., Matsui, S., Yokoyama, T., Kim, S.W., Hara, M., Hosono, H., 2012. Ammonia synthesis using a stable electride as an electron donor and reversible hydrogen store. *Nat. Chem.* 4 (11), 934–940. Article.
- Kitano, M., Inoue, Y., Sasase, M., Kishida, K., Kobayashi, Y., Nishiyama, K., Tada, T., Kawamura, S., Yokoyama, T., Hara, M., et al., 2018. Self-organized ruthenium-barium core-shell nanoparticles on a mesoporous calcium amide matrix for efficient low-temperature ammonia synthesis. *Angew. Chem. Int. Ed.* 57 (10), 2648–2652.
- Kobayashi, Y., Tang, Y., Kageyama, T., Yamashita, H., Masuda, N., Hosokawa, S., Kageyama, H., 2017. Titanium-based hydrides as heterogeneous catalysts for ammonia synthesis. *J. Am. Chem. Soc.* 139 (50), 18240–18246.
- Kobayashi, H., Hayakawa, A., Somarathne, K.D., Kunkuma, A., Okafor, Ekenechukwu, C., 2019. Science and technology of ammonia combustion. *Proc. Combust. Inst.* 37 (1), 109–133.
- Kojima, R., Aika, K., 2001. Cobalt molybdenum bimetallic nitride catalysts for ammonia synthesis Part 2. Kinetic study. *Appl. Catal. A-Gen.* 218 (1–2), 121–128.
- Kojima, Y., 2019. Hydrogen storage materials for hydrogen and energy carriers. *Int. J. Hydrog. Energy* 44 (33), 18179–18192.
- Lamb, K.E., Dolan, M.D., Kennedy, D.F., 2019. Ammonia for hydrogen storage; A review of catalytic ammonia decomposition and hydrogen separation and purification. *Int. J. Hydrog. Energy* 44 (7), 3580–3593.
- Lan, R., Irvine, J.T.S., Tao, S., 2012. Ammonia and related chemicals as potential indirect hydrogen storage materials. *Int. J. Hydrog. Energy* 37 (2), 1482–1494.
- Lin, B., Qi, Y., Wei, K., Lin, J., 2014. Effect of pretreatment on ceria-supported cobalt catalyst for ammonia synthesis. *RSC Adv.* 4 (72).
- Liu, H., 2013a. Ammonia Synthesis Catalysts: Innovation and Practice. Chemical Industry Press, World Scientific.
- Liu, H., 2013b. Ammonia Synthesis Catalysts: Innovation and Practice. World Scientific Publishing Company Pte Limited.
- Liu, H.Z., 2014. Ammonia synthesis catalyst 100 years: practice, enlightenment and challenge. *Chin. J. Catal.* 35 (10), 1619–1640. Review.
- Malmali, M., Le, G., Hendrickson, J., Prince, J., McCormick, A.V., Cussler, E.L., 2018. Better absorbents for ammonia separation. *ACS Sustain. Chem. Eng.* 6 (5), 6536–6546.
- Morlanés, N., Katikaneni, S.P., Paglieri, S.N., Harale, A., Solami, B., Sarathy, S.M., Gascon, J., 2021. A technological roadmap to the ammonia energy economy: current state and missing technologies. *Chem. Eng. J.* 408, 127310.
- Newton, R.H., 1935. Activity coefficients of gases. *Ind. Eng. Chem.* 27 (3), 302–306.
- Nicol, W., Hildebrandt, D., Glasser, D., 1998. Crossing reaction equilibrium in an adiabatic reactor system. *Dev. Chem. Eng. Miner. Process.* 6 (1–2), 41–54.
- Noshervani, S.A., Neto, R.C., 2021. Techno-economic assessment of commercial ammonia synthesis methods in coastal areas of Germany. *J. Energy Storage* 34, 102201.
- Ogawa, T., Kobayashi, Y., Mizoguchi, H., Kitano, M., Abe, H., Tada, T., Toda, Y., Niwa, Y., Hosono, H., 2018. High electron density on Ru in intermetallic YRu_2 : the application to catalyst for ammonia synthesis. *J. Phys. Chem. C* 122 (19), 10468–10475.
- Ogawa, T., 2022. Chapter 12 - ammonia as a carrier of renewable energy: recent progress of ammonia synthesis by homogeneous catalysts, heterogeneous catalysts, and electrochemical method. *Emerging Trends to Approaching Zero Waste*. Elsevier, pp. 265–291. Hussain, C. M., Singh, S., Goswami, L. Eds.
- Paul J. Faust Otto C. Pless, J. Startup procedure for the synthesis of ammonia. 1978. Peters, M.S., Timmerhaus, K.D., West, R.E., 2003. *Plant Design and Economics for Chemical Engineers*. McGraw-Hill Education.
- Rarogpilecka, W., Miskiewicz, E., Matyszek, M., Kaszkur, Z., Kepinski, L., Kowalczyk, Z., 2006. Carbon-supported cobalt catalyst for ammonia synthesis: effect of preparation procedure. *J. Catal.* 237 (1), 207–210.
- Rohr, B.A., Singh, A.R., Nørskov, J.K., 2019. A theoretical explanation of the effect of oxygen poisoning on industrial Haber-Bosch catalysts. *J. Catal.* 372, 33–38.
- Ronduda, H., Zybort, M., Patkowski, W., Ostrowski, A., Jodlowski, P., Szymanski, D., Kepinski, L., Rarog-Pilecka, W., 2021. A high performance barium-promoted cobalt catalyst supported on magnesium-lanthanum mixed oxide for ammonia synthesis. *RSC Adv.* 11 (23), 14218–14228.
- Rosowski, F., Hornung, A., Hinrichsen, O., Herein, D., Muhler, M., Ertl, G., 1997. Ruthenium catalysts for ammonia synthesis at high pressures: preparation, characterization, and power-law kinetics. *Appl. Catal. A* 151 (2), 443–460.
- Rossetti, L., Forni, L., 2005. Effect of Ru loading and of Ru precursor in Ru/C catalysts for ammonia synthesis. *Appl. Catal. A* 282 (1–2), 315–320.
- Rossetti, L., Pernicone, N., Ferrero, F., Forni, L., 2006. Kinetic study of ammonia synthesis on a promoted Ru/C catalyst. *Ind. Eng. Chem. Res.* 45 (12), 4150–4155.
- Sánchez, A., Martín, M., 2018a. Scale up and scale down issues of renewable ammonia plants: towards modular design. *Sustain. Prod. Consum.* 16, 176–192.
- Sánchez, A., Martín, M., 2018b. Optimal renewable production of ammonia from water and air. *J. Clean. Prod.* 178, 325–342.
- Saadatjou, N., Jafari, A., Sahebdehfar, S., 2015. Ruthenium nanocatalysts for ammonia synthesis: a review. *Chem. Eng. Commun.* 202 (4), 420–448.
- Sato, K., Miyahara, S.I., Tsujimaru, K., Wada, Y., Toriyama, T., Yamamoto, T., Matsumura, S., Inazu, K., Mohri, H., Iwasa, T., et al., 2021. Barium oxide encapsulating cobalt nanoparticles supported on magnesium oxide: active non-noble metal catalysts for ammonia synthesis under mild reaction conditions. *ACS Catal.* 11 (21), 13050–13061.
- Sgouridis, S., Carbajales-Dale, M., Csala, D., Chiesa, M., Bardi, U., 2019. Comparative net energy analysis of renewable electricity and carbon capture and storage. *Nat. Energy*.
- Shaw, H.R., Wones, D.R., 1964. Fugacity coefficients for hydrogen gas between 0 degrees and 1000 °C, for pressures to 3000 atm. *Am. J. Sci.* 262 (7), 918–929.
- Smith, A.R., Klosek, J., 2001. A review of air separation technologies and their integration with energy conversion processes. *Fuel Process. Technol.* 70 (2), 115–134.
- Supekar, S.D., Skerlos, S.J., 2015. Reassessing the efficiency penalty from carbon capture in coal-fired power plants. *Environ. Sci. Technol.* 49 (20), 12576–12584.
- Temkin, M., 1950. Kinetics of ammonia synthesis at high pressures. *Russ. J. Phys. Chem.* A 24 (24), 1312.
- The World's Most Expensive Fertilizer Market: Sub-Saharan Africa. *Gro Intelligence*, 2016. <https://gro-intelligence.com/insights/fertilizers-in-sub-saharan-africa> (accessed 2023 January 14th).
- Tsubame BHB Co., L. Technology /Business Introduction. 2022. <https://tsubame-bhb.co.jp/en/business-technology> (accessed 2023 January 14th).
- U.S. Energy Information Administration, Transportation sector energy consumption. *International Energy Outlook 2016*, 127–137.
- U.S. Energy Information Administration, Annual Energy Outlook 2020. 2020.
- U.S. Energy Information Administration, Electric Power Monthly with Data for June 2020. *Independent Statistics & Analysis* 2020.
- U.S. Geological Survey. *Mineral Commodity Summaries 2020*; 2020.
- Umicore, 2024. <https://pmm.umicore.com/en/prices/ruthenium/>(accessed).
- Wagner, K., Malmali, M., Smith, C., McCormick, A., Cussler, E.L., Zhu, M., Seaton, N.C.A., 2017. Column absorption for reproducible cyclic separation in small scale ammonia synthesis. *AIChE J.* 63 (7), 3058–3068.
- Wang, P., Chang, F., Gao, W., Guo, J., Wu, G., He, T., Chen, P., 2017. Breaking scaling relations to achieve low-temperature ammonia synthesis through LiH-mediated nitrogen transfer and hydrogenation. *Nat. Chem.* 9 (1), 64–70.
- Wang, Q., Pan, J., Guo, J., Hansen, H.A., Xie, H., Jiang, L., Hua, L., Li, H., Guan, Y., Wang, P., et al., 2021. Ternary ruthenium complex hydrides for ammonia synthesis via the associative mechanism. *Nat. Catal.* 4 (11), 959–967.
- Wickramasinghe, L.A., Ogawa, T., Schrock, R.R., Müller, P., 2017. Reduction of dinitrogen to ammonia catalyzed by molybdenum diamido complexes. *J. Am. Chem. Soc.* 139 (27), 9132–9135.
- Wijayanta, A.T., Oda, T., Purnomo, C.W., Kashiwagi, T., Aziz, M., 2019. Liquid hydrogen, methylcyclohexane, and ammonia as potential hydrogen storage: comparison review. *Int. J. Hydrog. Energy* 44 (29), 15026–15044.
- Woods, D.R., 2007. *Rules of Thumb in Engineering Practice*. Wiley-VCH Verlag GmbH & Co. KGaA. Book.
- Wu, J., Li, J., Gong, Y., Kitano, M., Inoshita, T., Hosono, H., 2019. Intermetallic electride catalyst as a platform for ammonia synthesis. *Angew. Chem. Int. Ed. Engl.* 58 (3), 825–829.
- Yandulov, D.V., Schrock, R.R., 2003. Catalytic reduction of dinitrogen to ammonia at a single molybdenum center. *Science* 301 (5629), 76–78 (1979).
- Ye, T.N., Park, S.W., Lu, Y., Li, J., Sasase, M., Kitano, M., Tada, T., Hosono, H., 2020. Vacancy-enabled N_2 activation for ammonia synthesis on a Ni-loaded catalyst. *Nature* 583 (7816), 391–395.
- Yoshida, M., Ogawa, T., Imamura, Y., Ishihara, K.N., 2021. Economies of scale in ammonia synthesis loops embedded with iron- and ruthenium-based catalysts. *Int. J. Hydrog. Energy* 46 (57), 28840–28854.
- Yuying, L. Centering, trust region, reflective techniques for nonlinear minimization subject to bounds; 1993.
- Zauba. India's import export data: detailed import data of synthesis catalyst 1. <https://www.zauba.com/import-SYNTHESIS+CATALYST+1-hs-code.htm> (accessed 2022 June 19th).
- Zhao, Y., Setzler, B.P., Wang, J., Nash, J., Wang, T., Xu, B., Yan, Y., 2019. An efficient direct ammonia fuel cell for affordable carbon-neutral transportation. *Joule*.
- Zybort, M., Tarka, A., Patkowski, W., Ronduda, H., Mierzwa, B., Kepinski, L., Rarog-Pilecka, W., 2022. Structure sensitivity of ammonia synthesis on cobalt: effect of the cobalt particle size on the activity of promoted cobalt catalysts supported on carbon. *Catalysts* 12 (10).